Dzyaloshinsky-Moriya-induced order in the spin-liquid phase of the $S=1/2$ pyrochlore antiferromagnet

Valeri N. Kotov,[1,*] Maged Elhajal,[2] Michael E. Zhitomirsky,[3] and Frédéric Mila[1]
[1]*Institute of Theoretical Physics, Swiss Federal Institute of Technology (EPFL), 1015 Lausanne, Switzerland*
[2]*Max-Planck-Institut für Mikrostrukturphysik, Weinberg 2, 06120 Halle, Germany*
[3]*Commissariat à l'Energie Atomique, DSM/DRFMC/SPSMS, 38054 Grenoble, France*
(Received 2 May 2005; published 11 July 2005)

We show that the $S=1/2$ pyrochlore lattice with both Heisenberg and antisymmetric Dzyaloshinsky-Moriya (DM) interactions can order antiferromagnetically into a state with chiral symmetry, dictated by the distribution of the DM interactions. The chiral antiferromagnetic state is characterized by a small staggered magnetic moment induced by the DM interaction. An external magnetic field can also lead to characteristic field-induced ordering patterns, strongly dependent on the field direction, and generally separated by a quantum phase transition from the chiral ordered phase. The phase diagram at finite temperature is also discussed.

DOI: 10.1103/PhysRevB.72.014421 PACS number(s): 75.10.Jm, 75.30.Et

I. INTRODUCTION

The behavior of many-body systems involving quantum spins has been one of the central topics in recent years because the properties of such systems are relevant to a great variety of materials, mostly oxides. The structure of the ground state and the various symmetry broken phases that emerge are issues of special interest, especially in systems of low dimensionality and/or where frustration is present.[1] In this context, the Heisenberg model on the three-dimensional (3D) pyrochlore lattice consisting of corner-sharing tetrahedra [shown in Fig. 1(a)], is in a league of its own. The pyrochlore lattice is strongly geometrically frustrated and is relevant to numerous compounds. It has been argued that no magnetic order is present in the ground state.[2–4] The effects of various additional interactions have also been studied, such as magnetoelastic couplings,[5] long-range dipolar interactions,[6] and orbital degeneracy.[7] These interactions (in addition to various anisotropies) can generally lead to bond, magnetic, and/or orbital order, and which of them is dominant depends on the details of the model relevant to the specific class of materials.

In the present work, we study a mechanism for magnetic order in the $S=1/2$ pyrochlore lattice, driven by the Dzyaloshinsky-Moriya (DM) interactions. In the pyrochlore, such interactions are expected to be present by symmetry. For the $S=1/2$ Heisenberg model on the pyrochlore lattice it has been suggested[2,4] that the ground state is dimerized (nonmagnetic), but macroscopic degeneracy still remains. For certain other lattices, such as the two-dimensional (2D) pyrochlore and related models,[8] the ground state is a unique valence-bond solid, and while the DM interactions (if present) can lead to nontrivial order in the ground state, such DM-induced order can only occur above a critical threshold, due to its inherent competition with the underlying dimer order.[8] In this work, we show that in the 3D pyrochlore antiferromagnet, where a macroscopic degeneracy is present, the DM interactions have a more profound effect and can lift the degeneracy, leading to a chiral antiferromagnetic state with a small staggered magnetic moment. In an external magnetic field, quantum transitions between weakly ordered states with different symmetries, depending on the field direction, are possible. We determine the field-induced patterns for several field orientations, generally pointing in highly symmetric crystal directions. The phase diagram at finite temperature is also briefly discussed.

The spin Hamiltonian ($S=1/2$) is

$$\hat{\mathcal{H}} = \sum_{\mathbf{i,j}} J_{\mathbf{i,j}} \mathbf{S_i} \cdot \mathbf{S_j} + \sum_{\mathbf{i,j}} \mathbf{D_{i,j}} \cdot (\mathbf{S_i} \times \mathbf{S_j}), \qquad (1)$$

where $\mathbf{D_{i,j}}$ are the DM vectors to be specified later. We start by summarizing the results for $\mathbf{D_{i,j}}=0$, i.e., the Heisenberg case. Our starting point is the strong-coupling approach, similar to that of Refs. 2 and 4, with the lattice divided into two interpenetrating sublattices, one of them formed by "strong" tetrahedra (with exchange J), connected by "weak" tetrahedra (exchange J'). The strong tetrahedra then form a fcc lattice, as shown in Fig. 2(a), where every site represents a tetrahedron, and one can attempt to analyze the structure of the ground state starting from the limit $J' \ll J$.

For $J'=0$ the tetrahedra are disconnected, and on a single tetrahedron the ground state is a singlet and is twofold degenerate. We choose the two ground states as $|s_1\rangle=(1/\sqrt{3}) \times\{[1,2][3,4]+[2,3][4,1]\}$, $|s_2\rangle=\{[1,2][3,4]-[2,3][4,1]\}$,

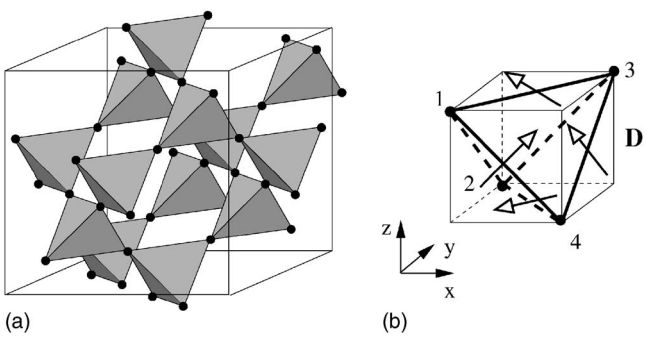

FIG. 1. (a) Pyrochlore lattice. (b) Distribution of DM vectors on a single tetrahedron (four of the six shown, see text).

where $[k,l]$ denotes a singlet formed by the nearest-neighbor spins k and l, labeled as in Fig. 1(b). In the pseudospin $T=1/2$ representation, so that $T_z=1/2$ corresponds to $|s_1\rangle$ and $T_z=-1/2$ corresponds to $|s_2\rangle$, one finds that the third order is the lowest one contributing to the effective intertetrahedron Hamiltonian in the singlet subspace[9]

$$\hat{\mathcal{H}}_{\rm eff}=\frac{J'^3}{8J^2}[\hat{\mathcal{H}}^{(2)}_{\rm eff}+\hat{\mathcal{H}}^{(3)}_{\rm eff}]+{\rm const}, \tag{2}$$

where

$$\hat{\mathcal{H}}^{(2)}_{\rm eff}=\sum_{\langle \mathbf{i},\mathbf{j}\rangle}\{\Omega^x_{\mathbf{ij}}T^x_{\mathbf{i}}T^x_{\mathbf{j}}+\Omega^z_{\mathbf{ij}}T^z_{\mathbf{i}}T^z_{\mathbf{j}}+\Omega^{xz}_{\mathbf{ij}}(T^x_{\mathbf{i}}T^z_{\mathbf{j}}+T^z_{\mathbf{i}}T^x_{\mathbf{j}})\}, \tag{3}$$

$$\hat{\mathcal{H}}^{(3)}_{\rm eff}=\sum_{(\mathbf{i},\mathbf{j},\mathbf{k})}\left\{\frac{1}{3}T^z_{\mathbf{i}}T^z_{\mathbf{j}}T^z_{\mathbf{k}}-T^z_{\mathbf{i}}T^x_{\mathbf{j}}T^x_{\mathbf{k}}+\frac{T^z_{\mathbf{i}}}{\sqrt{3}}(T^x_{\mathbf{j}}T^z_{\mathbf{k}}-T^z_{\mathbf{j}}T^x_{\mathbf{k}})\right\}. \tag{4}$$

In the two-body part, we have defined

$$\Omega^x_{03}=\Omega^x_{12}=1/2,\Omega^z_{03}=\Omega^z_{12}=-1/6,$$

$$\Omega^z_{23}=\Omega^z_{01}=\Omega^z_{02}=\Omega^z_{13}=1/3,$$

$$\Omega^{xz}_{23}=\Omega^{xz}_{01}=-\Omega^{xz}_{02}=-\Omega^{xz}_{13}=1/(2\sqrt{3}). \tag{5}$$

All remaining $\Omega_{\mathbf{ij}}=0$, $\mathbf{i}<\mathbf{j}$. The site indexes $\mathbf{i},\mathbf{j}$ refer to the fcc lattice made of individual tetrahedra, Fig. 2(a), and it is sufficient to know the interactions on one "supertetrahedron," shown in green (light gray) (containing the sites 0, 1, 2, and 3). In the three-body interaction, the indexes run over the values: $(\mathbf{i},\mathbf{j},\mathbf{k})=\{(3,2,1),(1,0,3),(2,3,0),(0,1,2)\}$.

On a mean-field level the ground state of $\hat{\mathcal{H}}_{\rm eff}$ is defined by the following averages:

$$\langle T^x_1\rangle=-\sqrt{3}/4,\quad \langle T^z_1\rangle=1/4,$$

$$\langle T^x_2\rangle=\sqrt{3}/4,\quad \langle T^z_2\rangle=1/4,$$

$$\langle T^x_3\rangle=0,\quad \langle T^z_3\rangle=-1/2,$$

$$\langle T^x_0\rangle=0,\quad \langle T^z_0\rangle=0. \tag{6}$$

This means that while a dimerization pattern sets in on sites 1–3, the pseudospins on the 0 sites, shown in blue (dark gray) in Fig. 2(a) remain "free," i.e., there is no fixed dimer pattern on those sites and consequently a macroscopic degeneracy remains.[4]

One should certainly keep in mind that the strong-coupling approach artificially breaks the lattice symmetry and while one hopes that the structure of the ground state is correct, even in the isotropic limit $J'=J$, it is very difficult to assess this by other means (e.g., exact diagonalizations) at the present time. Nevertheless this approach is expected to provide a reliable description of the ground-state properties as long as the relevant physics remain in the singlet subspace, i.e., the triplet modes stay high in energy and no magnetic order is generated, as might be the case for the pyrochlore antiferromagnet due to the strong frustration.

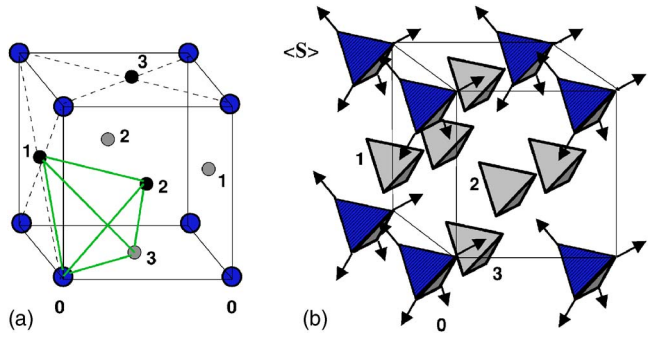

FIG. 2. (Color online) (a) A fcc lattice of tetrahedra (tetrahedron=dot) with interactions J' between them. (b) Antiferromagnetic chiral order on the blue (dark gray) tetrahedra, with magnetic moment $|\langle\mathbf{S}\rangle|\sim\tilde{D}$, induced by the DM interactions. On the gray tetrahedra (labeled as 1,2,3) the order has the same symmetry, but is much weaker $|\langle\mathbf{S}\rangle|\sim\tilde{D}^3\ll\tilde{D}$, Eq. (9), and is not shown.

Fluctuations around the mean-field solution, Eq. (6), can lift the degeneracy, leading to unique dimer order. However the corresponding degeneracy lifting energy scale is very small,[4] of the order of $10^{-3}\beta$, $\beta\equiv J'^3/(48J^2)$. A unique (singlet) ground state is also produced if one starts the expansion from a larger cluster of 16 sites, with an ordering energy scale (energy gain) of 10^{-2} J, extrapolated to the limit where all couplings are equal.[10]

In what follows, we will take the mean-field solution as a starting point and discuss a physical mechanism, based on the presence of interactions beyond Heisenberg exchange, that can lead to the lifting of degeneracy and consequently to (magnetic) order in the ground state.

II. CHIRAL ANTIFERROMAGNETIC ORDER INDUCED BY THE DZYALOSHINSKY-MORIYA INTERACTIONS

Now we consider the effect of the DM interactions[11,12] on the ground-state properties. On a single tetrahedron, the DM vectors are distributed as shown in Fig. 1(b), or explicitly: $\mathbf{D}_{13}=(D/\sqrt{2})(-1,1,0)$, $\mathbf{D}_{24}=(D/\sqrt{2})(-1,-1,0)$, $\mathbf{D}_{43}=(D/\sqrt{2})(0,-1,1)$, $\mathbf{D}_{12}=(D/\sqrt{2})(0,-1,-1)$, $\mathbf{D}_{14}=(D/\sqrt{2})(1,0,1)$, $\mathbf{D}_{23}=(D/\sqrt{2})(1,0,-1)$. Here D is the magnitude of the (all equal) DM vectors. The directions of the DM vectors respect the pyrochlore lattice symmetry and thus the DM interactions are expected to be always present in the system.[13] Because $\mathbf{D}_{ij}$ originate from the spin-orbit coupling,[11,12] we have $D\ll J,J'$, and typically the values of the DM interactions are several percentages of the Heisenberg couplings. There are two DM distribution patterns that are equally acceptable on symmetry grounds—the one shown in Fig. 1(b) and one with all directions of the vectors $\mathbf{D}_{ij}$ reversed ($\mathbf{D}_{ij}\rightarrow-\mathbf{D}_{ij}$). These two cases were named, respectively, "indirect" and "direct" in Ref. 13. The reader is referred to that paper for more details on Moriya's rules as applied to the pyrochlore lattice. In the extreme quantum case of $S=1/2$, and within our approach, we have found that the two allowed (by symmetry) DM distributions lead to qualitatively the same physics [see discussion following Eq. (8)].

Following the strong-coupling approach outlined above for the purely Heisenberg case, we have to determine how the singlet ground states $|s_1\rangle$ and $|s_2\rangle$ on a single tetrahedron are modified by the presence of D. Because the DM interactions break the spin rotational invariance, they admix triplets to the two ground states, not lifting their degeneracy.[8] We will also be interested in effects in the presence of an external magnetic field; in this case, the field (in combination with the DM interactions) also mixes certain triplet states with $|s_1\rangle$ and $|s_2\rangle$. In order to determine the additional contributions to $\hat{\mathcal{H}}_{\text{eff}}$, it is convenient to express the spin operators on a singlet tetrahedron, labeled as in Fig. 1(b), in terms of the pseudospin operators. For magnetic field $\mathbf{H}=(H/\sqrt{2})(1,1,0)$ (along the 1–3 bond), assuming $D \ll J$ and $H \ll J$, we obtain (defining the rescaled quantities $\tilde{D},\tilde{H}$ along the way)

$$\mathbf{H} = \frac{H}{\sqrt{2}}(1,1,0), \quad \tilde{D} \equiv D/J, \quad \tilde{H} \equiv H/J,$$

$$S^x_{1,3} = \mp \frac{2\tilde{D}}{\sqrt{6}} T^y - \frac{\tilde{D}\tilde{H}}{\sqrt{3}} T^x, \quad S^x_{2,4} = \mp \frac{2\tilde{D}}{\sqrt{6}} T^y + \frac{\tilde{D}\tilde{H}}{\sqrt{3}} T^x,$$

$$S^y_{1,3} = \mp \frac{2\tilde{D}}{\sqrt{6}} T^y + \frac{\tilde{D}\tilde{H}}{\sqrt{3}} T^x, \quad S^y_{2,4} = \pm \frac{2\tilde{D}}{\sqrt{6}} T^y - \frac{\tilde{D}\tilde{H}}{\sqrt{3}} T^x,$$

$$S^z_{1,3} = \frac{2\tilde{D}}{\sqrt{6}} T^y \mp \tilde{D}\tilde{H} T^z, \quad S^z_{2,4} = -\frac{2\tilde{D}}{\sqrt{6}} T^y \pm \frac{\tilde{D}\tilde{H}}{\sqrt{3}} T^x. \qquad (7)$$

The notation $\mathbf{S}_{i,j}$ simply combines in one line the formulas for both $\mathbf{S}_i$ and $\mathbf{S}_j$, where i and j label sites on a tetrahedron [as defined in Fig. 1(b)], while the left index in $\mathbf{S}_{i,j}$ corresponds to the upper sign on the right-hand side, and the right index, to the lower sign. The formulas in Eq. (7) are obtained by using the ground-state wave functions, written explicitly in Ref. 8 [Eqs. (2) and (5)], to lowest order in $\tilde{D}$ and $\tilde{D}\tilde{H}$. For magnetic field in the z direction, the corresponding expressions are given in Appendix A.

First we analyze the case of zero magnetic field ($\mathbf{H}=0$). Taking into account the connections between the tetrahedra [green (light gray) bonds in Fig. 2(a)], and using Eq. (7), we obtain an additional interaction term, so that the full effective Hamiltonian $\hat{\mathcal{H}}^{(DM)}_{\text{eff}}$ becomes

$$\hat{\mathcal{H}}^{(DM)}_{\text{eff}} = \hat{\mathcal{H}}_{\text{eff}} - J'\tilde{D}^2 \frac{2}{3} \sum_{\mathbf{i}<\mathbf{j}} T^y_{\mathbf{i}} T^y_{\mathbf{j}}, \qquad (8)$$

where $\hat{\mathcal{H}}_{\text{eff}}$ is the part originating from the Heisenberg exchanges, Eq. (2). The above result is obtained in the lowest first order in J'. While extra terms of the same power $J'(D'/J)^2$ also arise from the DM interactions D' on the intertetrahedral bonds, we find that they only give a small renormalization of the energy scale $J'^3/(8J^2)$ in Eq. (2) and, therefore, are neglected.

We would like to also point out that, in general, the coupling constant in $\hat{\mathcal{H}}^{(DM)}_{\text{eff}}$ is not symmetric under $D \to -D$. To verify this requires a calculation of the next-to-leading order in $\tilde{D}$ in Eq. (7). We have found that, in the case of zero field $H=0$, the next order present is $\tilde{D}^2$, and one has to substitute in all formulas $\tilde{D} \to \tilde{D} - [(3/4\sqrt{2})\tilde{D}^2]$. Consequently the same substitution has to be made in the coefficient $-J'\tilde{D}^2\frac{2}{3}$ in Eq. (8). However, most importantly the $T^y_{\mathbf{i}} T^y_{\mathbf{j}}$ structure of the interaction is not affected by increasing the strength of $\tilde{D} \ll 1$, and from now on we will work with the leading order in $\tilde{D}$. Therefore the physics (ground-state structure) associated with the two DM distribution patterns will be the same. This conclusion might be connected with the fact that we have kept only the lowest nontrivial order in the coupling J' in the effective Hamiltonian—we have used this as our guiding principle as the difficulties associated with the derivation and analysis of higher orders seem insurmountable.

We have performed mean-field calculations of the Hamiltonian defined by Eqs. (2)–(4) and (8) in the unit cell of Fig. 2(a), as represented by the four sites connected by green (light gray) lines. The results can be simply summarized in the limit $\tilde{D} \ll 1$, which is also the case of physical relevance. It is physically clear that ferromagnetic order in the $T^y_{\mathbf{i}}$ component is generated on the 0 sites, because no order in the $T^{x,z}_{\mathbf{i}}$ components (dimer order) was present on those sites without DM interactions (on mean-field level), Eq. (6). Indeed we find $\langle T^y_0 \rangle = 1/2$, while for the other sites we have, to lowest nontrivial order in D, $\langle T^y_{\mathbf{i}} \rangle \approx 1.8(D/J')^2$, $\mathbf{i}=1,2,3$. From Eq. (7), it is then clear that a nonzero average of the operator $T^y_{\mathbf{i}}$ corresponds to a finite moment in the ground state, with magnitude $|\langle \mathbf{S} \rangle_{\mathbf{i}}| = \tilde{D}\sqrt{2}\langle T^y_{\mathbf{i}} \rangle$. To summarize

$$\langle T^y_0 \rangle = 1/2, \quad \langle T^y_{\mathbf{i}} \rangle \approx 1.8\frac{D^2}{J'^2}, \quad \mathbf{i}=1,2,3 \Rightarrow |\langle \mathbf{S} \rangle_{\mathbf{i}}| = \frac{\tilde{D}}{\sqrt{2}}, \quad \mathbf{i}=0, \quad |\langle \mathbf{S} \rangle_{\mathbf{i}}| \approx \frac{3.6}{\sqrt{2}}\tilde{D}\frac{D^2}{J'^2}, \quad \mathrm{i}=1,2,3. \qquad (9)$$

Here $|\langle \mathbf{S} \rangle_{\mathbf{i}}|$ stands for the magnitude of the moment on each site of pyrochlore lattice, belonging to a tetrahedron labeled by the index $\mathbf{i}$. From Eq. (7), it follows that the moments point out of the cube's center [the cube is defined in Fig. 1(b)], leading to formation of sublattices and the order shown in Fig. 2(b). Because from Eq. (9), $|\langle \mathbf{S} \rangle_{\mathbf{i}}|/|\langle \mathbf{S} \rangle_0| \sim (D/J')^2 \ll 1$, $i=1,2,3$, we have neglected the magnetic order on those tetrahedra.

The antiferromagnetic order of Fig. 2(b) corresponds to nonzero scalar chirality $\chi=\langle \mathbf{S}_m\cdot(\mathbf{S}_n\times\mathbf{S}_l)\rangle\neq 0$, where m,n,l are any three spins on a given tetrahedron. The Ising symmetry $T^y_{\mathbf{i}}\to -T^y_{\mathbf{i}}$ is spontaneously broken in the ground state, which in terms of real spins corresponds to the time-reversal symmetry broken state of Fig. 2(b). In this state, the two ground-state wave functions $|\Phi\rangle$ and $|\Psi\rangle$ [see Eq. (A1)] form linear combinations in the "chiral" sector: $\alpha|\Phi\rangle+i\beta|\Psi\rangle$, where α,β are real coefficients $(\alpha^2+\beta^2=1)$. This combination is ferromagnetically repeated on every T^y ordered tetrahedron. A straightforward calculation shows that both $\langle T^y_{\mathbf{i}}\rangle \propto \alpha\beta$, $\chi\propto\alpha\beta$. The energy gain [per site of Fig. 2(a)] from the formation of the ordered state is $\Delta E=\langle\hat{\mathcal{H}}^{(DM)}_{\text{eff}}\rangle-\langle\hat{\mathcal{H}}_{\text{eff}}\rangle \approx -1.8J'\tilde{D}^2(D/J')^2$. The order we have just discussed is in competition with other mechanisms for lifting of the degeneracy that could originate from the Heisenberg interactions themselves (e.g., fluctuations beyond the mean field), typically also leading to very small energy scales.[4]

III. MAGNETIC ORDER INDUCED BY EXTERNAL MAGNETIC FIELDS IN THE PRESENCE OF DM INTERACTIONS

In the presence of an external magnetic field, other possibilities for lifting of the degeneracy exist. We will consider three symmetric field orientations, for which the results are particularly transparent. The magnetic field generally leads to splitting of the ground states, which in the language of the pseudospins produces an on-site "effective magnetic field" h in the pseudospin z direction. The effective Hamiltonian has the form

$$\hat{\mathcal{H}}^{(H)}_{\text{eff}}=\hat{\mathcal{H}}^{(DM)}_{\text{eff}}+h\sum_{\mathbf{i}}T^z_{\mathbf{i}}+\delta\hat{\mathcal{H}}^{(H)}_{\text{eff}}. \tag{10}$$

We consider fields in the (1, 1, 1), and (0, 0, 1) directions, as well as comment on the case (1, 1, 1), where the axes are defined in Fig. 1(b). Using the wave functions in a field, we obtain [see Eq. (A3)]

$$h=\begin{cases}\frac{1}{2}D^2H^2/J^3, & \mathbf{H}=\frac{H}{\sqrt{2}}(1,1,0)\\ -D^2H^2/J^3, & \mathbf{H}=H(0,0,1)\\ 0, & \mathbf{H}=\frac{H}{\sqrt{3}}(1,1,1).\end{cases} \tag{11}$$

$\delta\hat{\mathcal{H}}^{(H)}_{\text{eff}}$ in Eq. (10) represents lattice contributions, originating from the various combinations in Eq. (7) once the tetrahedra are coupled, and also producing terms of order D^2H^2. These terms are cumbersome and are not explicitly written, but their effect is taken into account in the (numerical) mean-field implementation within the unit cell of Fig. 2(a). A further discussion appears in Appendix B.

We will mostly discuss the two cases with $h\neq 0$. Then the on-site h term in Eq. (10) is responsible for the main effect, namely competition between order in the $T^z_{\mathbf{i}}$ pseudospin component and order in the chiral $T^y_{\mathbf{i}}$ component favored by Eq. (8). Therefore, the physics is that of the transverse field Ising model (although in our case the unit cell is larger). It is also clear that the mentioned competition is most effective on the "0" (blue or dark gray) sites, while the nonzero averages of $T^{z,x}_{\mathbf{i}}$ on the other sites are not much affected by the presence of small D and H. We have found that a quantum transition takes place between a state with $\langle T^y_0\rangle\neq 0, H<H_c$, and $\langle T^y_0\rangle=0, H\geq H_c$. The result for $\tilde{D}\ll 1$ can be written in an explicit way, and we have for the field $\mathbf{H}=(H/\sqrt{2})(1,1,0)$

$$\langle T^y_0\rangle^2=\frac{1}{4}\left[1-\left(\frac{\tilde{H}}{\tilde{H}_c}\right)^4\right],\quad \tilde{H}\leq\tilde{H}_c\approx 5.3\sqrt{\frac{J}{J'}}\tilde{D}, \tag{12}$$

$$\langle T^z_0\rangle^2=1/4-\langle T^y_0\rangle^2 \tag{13}$$

(and $\langle T^z_0\rangle<0$ since $h>0$). The values of the spin moments for given values of $\langle T^{x,y,z}_{\mathbf{i}}\rangle$ on a tetrahedron can be determined directly from Eq. (7). On the "0" (blue or dark gray) sites this leads to evolution of the magnetic order as shown in Figs. 3(a)–3(c). For $H=0$ there is only chiral order (blue or dark gray arrows) with moment $|\langle\mathbf{S}\rangle|\sim\tilde{D}$, changing, for $H>0$ into a combination of chiral-induced and field-induced order (red arrows) with $|\langle\mathbf{S}\rangle|\sim\tilde{D}\tilde{H}$. Gradually, as H approaches H_c, the chiral order diminishes [Eq. (12)], leaving for $H>H_c$ only the field-induced component, equal to $|\langle\mathbf{S}\rangle| =\tilde{D}\tilde{H}|\langle T^z_0\rangle|=\tilde{D}\tilde{H}/2$, $H>H_c$.

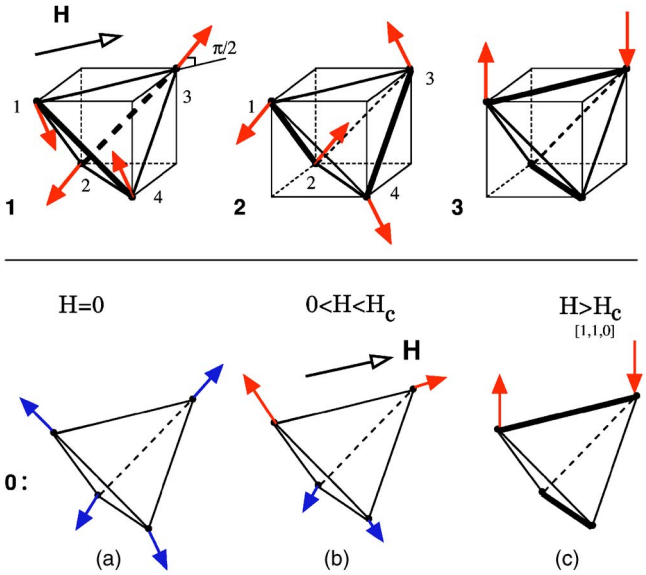

FIG. 3. (Color online) (a), (b), and (c) Evolution of magnetic order on the blue (dark gray) tetrahedra of Fig. 2(b) in an external magnetic field in the (1, 1, 0) direction. Upper row: field-induced order on the rest of the tetrahedra. The tetrahedra are labeled 0,1,2,3 as in Figs. 2(a) and 2(b). Blue (dark gray) arrows in (a) and (b) correspond to moments $|\langle\mathbf{S}\rangle|\sim\tilde{D}$, while the red (light gray) arrows on the upper row and (b) and (c) are the field- induced moments $|\langle\mathbf{S}\rangle|\sim\tilde{D}\tilde{H}$.

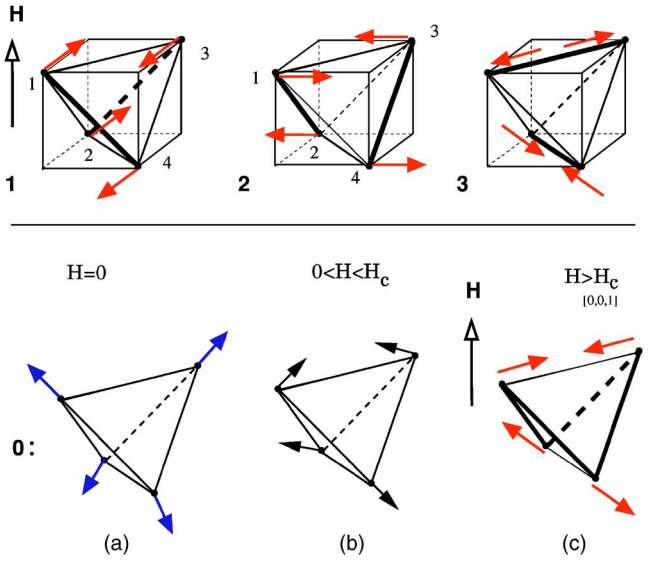

FIG. 4. (Color online) Same as Fig. 3, but for an external magnetic field in the (0, 0, 1) direction. Blue (dark gray) arrows in (a) correspond to the DM-induced order with $|\langle \mathbf{S} \rangle| \sim \tilde{D}$, red (light gray) arrows on the upper row and (c) correspond to the field-induced component $|\langle \mathbf{S} \rangle| \sim \tilde{D}\tilde{H}$, and black arrows in (b) are a mixture of the two.

On the tetrahedra 1, 2, 3 labeled as in Figs. 2(a) and 2(b), there is virtually no evolution as a function of the field, and the order is determined by Eq. (7) with $\langle T_{\mathbf{i}}^{x,z} \rangle$ fixed by the Heisenberg exchanges, see Eq. (6). This leads to the magnetic moments (proportional to $\tilde{D}\tilde{H}$) shown in Fig. 3, upper row. On tetrahedra 1 and 2, the spins point along the internal diagonals of the cube perpendicular to the field. Dimerization is also present in the ground state (bolder lines equal stronger bonds) and coexists with the magnetic order.

A similar quantum transition takes place for the magnetic field in the z direction $\mathbf{H}=H(0,0,1)$. In this case, the formulas in Eq. (A2) from Appendix A have to be used, and the field-induced order is shown in Fig. 4. The critical field is also somewhat smaller in this case $\tilde{H}_c \approx 3.8(J/J')^{1/2}\tilde{D}$, mainly due to the fact that h is larger by a factor of 2, see Eq. (11). For other, less symmetric field directions, the form of the effective Hamiltonian, and consequently the field-induced patterns, can be quite complex. Finally, in the case of a field $\mathbf{H} \sim (1,1,1)$, when $h=0$, the quantum transition described above does not take place, and the chiral order of Fig. 3(a) essentially does not evolve. In this case, the various additional terms similar to the ones described in Appendix B may lead to small, subleading deviations from the perfect chiral sate.

In addition to the field-induced ordered patterns of Fig. 3 and Fig. 4, determined mostly by the intertetrahedral interactions, a single tetrahedron with DM interactions also possesses a finite moment in the direction of the field,[8] meaning that the spins in Fig. 3 and Fig. 4 would also tend to tilt in that direction. However, the moment along the field is proportional to $\tilde{D}^2\tilde{H}$, as can be deduced from the fact that the ground-state energy varies as $\tilde{D}^2\tilde{H}^2$ from Eq. (A3). Consequently, this component has not been taken into account in Eqs. (7) and (A2), valid to the lowest order in $\tilde{D},\tilde{H}$. Finally, we emphasize that while we have assumed $\tilde{D},\tilde{H}$ to be small, the ratio $\tilde{D}/\tilde{H}$ can be arbitrary, meaning that the quantum transitions in a field are within the limit of validity of our approach.

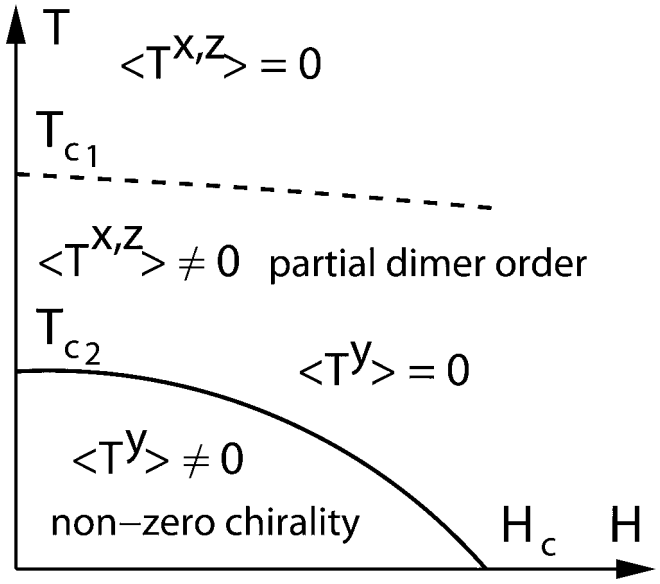

FIG. 5. Schematic phase diagram at nonzero temperature in the presence of small magnetic field ($H \ll J$) and DM interactions.

IV. PHASE DIAGRAM AND DISCUSSION

At finite temperature we expect the phase diagram to look as presented in Fig. 5 (it is assumed that $h \neq 0$). The higher transition temperature $T_{c1} \sim J'^3/J^2$ corresponds to the scale below which the translational symmetry is broken (dimerization occurs) and is determined by the energy scale in $\hat{\mathcal{H}}_{\text{eff}}$ for $D=0$, Eq. (2). We expect T_{c1} to have weak dependence on the magnetic field when DM interactions are present. At a lower scale T_{c2}, the Ising $T^y \to -T^y$ symmetry is spontaneously broken by Eq. (8). For $H=0$, we can estimate $T_{c2} \sim J'\tilde{D}^2(D/J')^2$. At a fixed field, this finite-temperature transition is in the 3D Ising universality class, and the specific heat diverges as $C \sim |T - T_{c2}(H)|^{-\alpha}$, $\alpha \approx 0.11$.[14] We emphasize that Fig. 5 shows only the low-field part of the phase diagram (since $H_c \sim D \ll J$), while the physics at high fields cannot be determined within the effective Hamiltonian framework presented here.

In certain pyrochlores, such as the gadolinium titanium oxides with $S=7/2$, field-driven phase transitions have been observed,[15] although in this material, the magnetic order is typically explained as originating from the long-range dipolar interactions. For such a large value of the spin the DM mechanism for magnetic order, at least the way it is developed in this work, should not be effective because our calculations were based on strong singlet correlations in the ground state. At the moment, it is hard to point out a class of materials where the DM interactions are definitely expected

to be dominant with respect to other anisotropies able to produce ordering; some possible examples are given in Ref. 13. In particular, our results are specific to the case $S=1/2$, while most currently known pyrochlores have higher S. Let us also point out the main differences between the present work and the purely classical model.[13] (a) We have found that the antiferromagnetic order is weak, determined by the DM interaction scale itself. (b) The chiral noncoplanar pattern is the stable one for $S=1/2$ in the absence of a field. Field-induced patterns then dominate for $H>H_c\sim D$. Let us also give some estimates: if we take the optimistic viewpoint and apply our formulas to the case $J=J'$, and take $J\sim 100$ K, $D/J\sim 10^{-1}$, then the characteristic temperature for onset of chiral order would be $T_{c2}\sim 10$ mK, and the magnitude of the moment $|\langle \mathbf{S}\rangle|\sim 0.1$. The characteristic critical fields would be $H_c\sim 10$ K. These should be viewed as the order of magnitude estimates. Inevitably, the scale T_{c2} falls into the mK range, which, in combination with the smallness of $\langle \mathbf{S}\rangle$ itself, would probably make the chiral state rather hard to observe with neutron scattering techniques used to probe the spin structure.[16] The spectral weight of magnetic excitations in such neutron scattering measurements would be determined by D itself. However, the scale of H_c of around $10T$ or smaller (also determined by D), means that the various field-induced patterns, strongly dependent on the magnetic field direction, might be accessible.

In conclusion, we have shown that DM interactions can induce weak antiferromagnetic order characterized by nonzero chirality. In an external magnetic field, quantum transitions between the chiral state and field-induced ordered states take place. Field-induced patterns with different symmetries, depending on the direction of the field, are very characteristic of the presence of DM interactions. We have used an expansion around a configuration that breaks the lattice symmetry[4] and leaves a macroscopic degeneracy, subsequently lifted by the DM interactions. Full restoration of lattice symmetry within such an approach seems impossible to achieve, as it is impossible for example in the large-N approach.[17] Nevertheless, we expect that without DM interactions, the ground-state properties and the inherent degeneracy present in this strongly frustrated magnet are well accounted for. In this situation, the DM interactions push the pyrochlore lattice toward the ordered states analyzed in the present work. More generally, the DM interactions can be relevant and lead to weak antiferromagnetism in strongly frustrated systems, where the Heisenberg exchanges on their own fail to produce long-range order. We also emphasize that the physics behind the weakly antiferromagnetic states with different symmetries discussed in this work is very different from the phenomenon of weak ferromagnetism, usually associated with DM interactions.

ACKNOWLEDGMENTS

Stimulating discussions with H. Tsunetsugu, O. Tchernyshyov, and C. Lhuillier, and the financial support of the Swiss National Fund and MaNEP (V.N.K. and F.M.) are gratefully acknowledged.

APPENDIX A: SPIN OPERATORS AND ENERGY LEVELS IN MAGNETIC FIELD

Here we present the expressions for the spin operators for the magnetic field in the z direction. The two ground-state wave functions $|s_1\rangle$, $|s_1\rangle$ are modified in the following way in the presence of DM interactions ($|s_1\rangle\rightarrow|\Phi\rangle, |s_2\rangle\rightarrow|\Psi\rangle$):

$$\mathbf{H}=H(0,0,1),$$

$$|\Phi\rangle=|s_1\rangle+\frac{i\sqrt{6}\tilde{D}}{4}[|p_x\rangle-|p_y\rangle+|q_x\rangle+|q_y\rangle]$$

$$+\frac{\sqrt{6}\tilde{D}\tilde{H}}{4}[|p_x\rangle+|p_y\rangle-|q_x\rangle+|q_y\rangle],$$

$$|\Psi\rangle=|s_2\rangle+\frac{i\tilde{D}}{2\sqrt{2}}[|p_x\rangle+|p_y\rangle+|q_x\rangle-|q_y\rangle]+i\tilde{D}|t_z\rangle$$

$$+\frac{\tilde{D}\tilde{H}}{2\sqrt{2}}[-|p_x\rangle+|p_y\rangle+|q_x\rangle+|q_y\rangle], \tag{A1}$$

where $|p_\mu\rangle$, $|q_\mu\rangle$, $|t_\mu\rangle$, $\mu=x,y,z$ are the three excited triplet states on a tetrahedron. From these equations we obtain

$$S^x_{1,3}=\mp\frac{2\tilde{D}}{\sqrt{6}}T^y\pm\frac{\tilde{D}\tilde{H}}{\sqrt{2}}T^z\pm\frac{\tilde{D}\tilde{H}}{\sqrt{6}}T^x,$$

$$S^y_{1,3}=\mp\frac{2\tilde{D}}{\sqrt{6}}T^y\pm\frac{\tilde{D}\tilde{H}}{\sqrt{2}}T^z\mp\frac{\tilde{D}\tilde{H}}{\sqrt{6}}T^x,$$

$$S^z_{1,3}=\frac{2\tilde{D}}{\sqrt{6}}T^y,$$

$$S^x_{2,4}=\mp\frac{2\tilde{D}}{\sqrt{6}}T^y\mp\frac{\tilde{D}\tilde{H}}{\sqrt{2}}T^z\mp\frac{\tilde{D}\tilde{H}}{\sqrt{6}}T^x,$$

$$S^y_{2,4}=\pm\frac{2\tilde{D}}{\sqrt{6}}T^y\pm\frac{\tilde{D}\tilde{H}}{\sqrt{2}}T^z\mp\frac{\tilde{D}\tilde{H}}{\sqrt{6}}T^x,$$

$$S^z_{2,4}=-\frac{2\tilde{D}}{\sqrt{6}}T^y. \tag{A2}$$

We also give the ground-state energy splitting on a single tetrahedron, in (weak) external magnetic field with arbitrary direction

$$\mathbf{H}=(H_x,H_y,H_z),$$

$$E_0^{(1,2)}=-\frac{3J}{2}-\frac{3D^2}{2J}-\frac{D^2|\mathbf{H}|^2}{J^3}$$

$$\pm\frac{D^2}{2J^3}\sqrt{|\mathbf{H}|^4-3(H_x^2H_y^2+H_x^2H_z^2+H_z^2H_y^2)}. \tag{A3}$$

From here the effective magnetic field h, appearing in the pseudospin Hamiltonian in Eq. (10), is $h=E_0^{(2)}-E_0^{(1)}$.

APPENDIX B: EFFECTIVE HAMILTONIAN CONTRIBUTIONS IN MAGNETIC FIELD

We briefly discuss the structure and treatment of the term $\delta\hat{\mathcal{H}}_{\rm eff}^{(H)}$ in Eq. (10). As is clear from Eqs. (7) and (A2), potential contributions of two types appear: (a) terms of the order $\tilde{D}^2\tilde{H}$, and (b) terms of the order $\tilde{D}^2\tilde{H}^2$. While treating these terms, we will assume that the unit cell structure of Fig. 2(a) does not change. Indeed, because we are interested in the case of weak fields $\tilde{H}\ll 1$, the above coupling constants are of the subleading order with respect to the case without a field, and therefore one does not expect the unit cell to change. Under this assumption, we find that the terms of order $\tilde{D}^2\tilde{H}$ vanish identically for the field directions considered in this work. The remaining contribution, e.g., for a field $\mathbf{H}=(H/\sqrt{2})(1,1,0)$, written (per site) within the unit cell of Fig. 2(a) is

$$\langle\delta\hat{\mathcal{H}}_{\rm eff}^{(H)}\rangle=\frac{J'}{6}\tilde{D}^2\tilde{H}^2\delta\hat{\mathcal{H}}, \tag{B1}$$

where

$$\delta\hat{\mathcal{H}}=-4(T_0^x+T_3^x)(T_1^x+T_2^x)+\sqrt{3}(T_0^x-T_3^x)(T_1^z-T_2^z)+\sqrt{3}(T_0^z-T_3^z)(T_1^x-T_2^x)+3(T_0^xT_3^x-T_0^zT_3^z+T_1^xT_2^x-T_1^zT_2^z). \tag{B2}$$

These terms were taken into account in our numerical solution of the mean-field equations corresponding to Eq. (10).

*Corresponding author. Electronic address: valeri.kotov@epfl.ch

[1] G. Misguich and C. Lhuillier in *Frustrated Spin Systems*, edited by H. T. Diep (World-Scientific, Singapore, 2003).
[2] A. B. Harris, A. J. Berlinsky, and C. Bruder, J. Appl. Phys. **69**, 5200 (1991).
[3] R. Moessner and J. T. Chalker, Phys. Rev. Lett. **80**, 2929 (1998); B. Canals and C. Lacroix, *ibid.* **80**, 2933 (1998).
[4] H. Tsunetsugu, Phys. Rev. B **65**, 024415 (2002).
[5] O. Tchernyshyov, R. Moessner, and S. L. Sondhi, Phys. Rev. B **66**, 064403 (2002).
[6] S. E. Palmer and J. T. Chalker, Phys. Rev. B **62**, 488 (2000).
[7] H. Tsunetsugu and Y. Motome, Phys. Rev. B **68**, 060405(R) (2003); O. Tchernyshyov, Phys. Rev. Lett. **93**, 157206 (2004).
[8] V. N. Kotov, M. E. Zhitomirsky, M. Elhajal, and F. Mila, Phys. Rev. B **70**, 214401 (2004).
[9] Our choice of ground states is different from that of Ref. 4 leading to different coefficients in $\hat{\mathcal{H}}_{\rm eff}$.
[10] E. Berg, E. Altman, and A. Auerbach, Phys. Rev. Lett. **90**, 147204 (2003).
[11] I. Dzyaloshinsky, J. Phys. Chem. Solids **4**, 241 (1958).
[12] T. Moriya, Phys. Rev. **120**, 91 (1960).
[13] M. Elhajal, B. Canals, R. Sunyer, and C. Lacroix, Phys. Rev. B **71**, 094420 (2005). This work considers the classical limit of the model.
[14] R. Guida and J. Zinn-Justin, J. Phys. A **31**, 8103 (1998).
[15] A. P. Ramirez, B. S. Shastry, A. Hayashi, J. J. Krajewski, D. A. Huse, and R. J. Cava, Phys. Rev. Lett. **89**, 067202 (2002); O. A. Petrenko, M. R. Lees, G. Balakrishnan, and D. McK Paul, Phys. Rev. B **70**, 012402 (2004); O. Cepas and B. S. Shastry, *ibid.* **69**, 184402 (2004).
[16] S.-H. Lee, C. Broholm, W. Ratcliff, G. Gasparovich, Q. Huang, T. H. Kim, and S.-W. Cheong, Nature (London) **418**, 856 2002).
[17] O. Tchernyshyov, R. Moessner, and S. L. Sondhi, cond-mat/0408498 (unpublished).